

Article

Enhancing Thermal Insulation of Geothermal Well Cement Using Alkali-Activated Straw Ash and Natural Zeolite

Ying Ji ^{1,*} , Qianqian Sha ¹, Gang Zhu ², Yuze Xue ^{3,4} and Tinghui Zhang ^{3,4}

¹ School of Materials Science and Engineering, Xi'an University of Architecture and Technology, Xi'an 710055, China; shaqianqian@xauat.edu.cn

² China Building Materials Industry Construction Xi'an Engineering Limited Company, Xi'an 710075, China; cbmxe2023@163.com

³ Key Laboratory of Coal Resources Exploration and Comprehensive Utilization, Ministry of Natural Resources, Xi'an 710021, China; xyz-88111@163.com (Y.X.); xiaot1943@126.com (T.Z.)

⁴ Shaanxi Coal Geology Group Co., Ltd., Xi'an 710021, China

* Correspondence: jiyiing@xauat.edu.cn

Abstract: To improve the heat extraction efficiency from the wellbore fluids to the stratum in the geothermal well, thermal insulation cement, which is prepared by alkali-excited straw ash-natural zeolite, was based on the orthogonal test. The properties of thermal insulation cement, such as compressive strength, thermal conductivity and fluidity, were tested, and the comprehensive evaluation and range analysis of thermal insulation cement were carried out by using analytic hierarchy process (AHP) as a macro reference index. The results show that the alkali equivalent of natural zeolite and water glass are the two biggest factors affecting the properties of cement. The compressive strength of the optimal mixture at 38 °C and 60 °C for 8 h is 9.26 MPa and 24.46 MPa, respectively, and the thermal conductivity reduction rates at 30 °C, 60 °C and 90 °C are 42.41%, 50.29% and 54.03%, respectively. The initial consistency of the optimal mixture is 13.9 BC and the consistency time is 123 min, which can be used for engineering cementing. In addition, the thickening time of cement can be adjusted according to water-reducing agent and retarder to meet the actual construction requirements of cementing.

Keywords: thermal insulation cement; thermal conductivity; compressive strength; thickening time; alkali excitation; straw ash; natural zeolite



Citation: Ji, Y.; Sha, Q.; Zhu, G.; Xue, Y.; Zhang, T. Enhancing Thermal Insulation of Geothermal Well Cement Using Alkali-Activated Straw Ash and Natural Zeolite. *Coatings* **2024**, *14*, 507. <https://doi.org/10.3390/coatings14040507>

Academic Editor: Edoardo Proverbio

Received: 27 March 2024

Revised: 12 April 2024

Accepted: 17 April 2024

Published: 19 April 2024



Copyright: © 2024 by the authors. Licensee MDPI, Basel, Switzerland. This article is an open access article distributed under the terms and conditions of the Creative Commons Attribution (CC BY) license (<https://creativecommons.org/licenses/by/4.0/>).

1. Introduction

As a green and clean energy, geothermal energy has a good development potential. However, in the process of geothermal energy exploitation, the heat loss in the middle and upper part of geothermal wells is a major challenge in geothermal energy exploitation [1]. In the middle and upper sections of the geothermal well, temperature of the geothermal fluids in the wellbore is higher than that of the stratum [2]. Heat energy is transferred from the geothermal fluids to the stratum, causing heat loss and resulting in lower wellhead temperatures [3–6]. The outlet temperature of geothermal fluids is a significant basis for determining the applications of geothermal energy [7]. Heat loss will reduce the application rate of geothermal energy and increase the costs of geothermal production. Therefore, it is necessary to reduce the thermal conductivity of the cement, to minimize the heat transfer from the geothermal fluids to the stratum [8]. Previous studies have shown that the use of insulating cement in the middle and upper part of geothermal wells can effectively reduce the heat loss of geothermal energy, thereby increasing the extraction rate of geothermal energy [9,10].

At present, many scholars have studied the use of thermal insulation materials, instead of part of the cement, to prepare thermal insulation cement used in the middle and upper parts of geothermal wells, such as those prepared by mixing a certain amount of fly ash [11],

rice husk ash [12], metakaolin and Silica fume [13], foams and hollow glass beads [14], instead of a part of cement. In addition, Zhou W [14] found that while filling foam hollow microbeads as insulation material to prepare cement paste can reduce the thermal conductivity of cement paste to $0.3719 \text{ W}/(\text{m}\cdot\text{K})$, the compressive strength of cement paste is reduced. Du Y [15] found that 0–25% of waste glass powder and limestone powder can significantly reduce the thermal conductivity of cement, and the thermal insulation effect of limestone powder is better than that of waste glass powder.

However, most of the traditional thermal insulation materials are lightweight and porous, which only improve the thermal insulation properties of cement while neglecting its mechanical properties. At present, using aerogels and alkali excitation materials as new thermal insulation materials can improve the problem of low compressive strength of traditional thermal insulation materials. Alaa Rashad M [16] found that gel insulation materials with low thermal conductivity and good compressive strength could be prepared by combining fly ash, metakaolin, hydrated lime and gypsum with a small amount of silica fume and graphite. Jadhav P S [17] found that adding 50% aerogel to biomass wheat straw can effectively reduce the thermal conductivity of the composite material and improve its thermal insulation and mechanical properties. An L. [18] found that the use of aerogel and ceramics to prepare ceramic nanocomposites has good high temperature resistance, and the thermal conductivity is only $0.024 \text{ W}/(\text{m}\cdot\text{K})$. Aerogel is incorporated into cement-based materials as thermal insulation material, although it can improve the mechanical properties and thermal insulation properties of cement at the same time, but the use cost is high and the durability is poor.

Scholars at home and abroad have carried out a lot of research on foam insulation materials, and found that the use of water glass-based foam materials as insulation materials can improve the thermal insulation performance while ensuring the mechanical properties of cement-based materials. Rong X [19] used fly ash, foam, aerogel and polypropylene fiber as raw materials to study alkali-excited aerogel foamed concrete with excellent thermal insulation properties and mechanical strength. The results show that fly ash can replace part of cement; adding aerogel and foam to concrete can significantly reduce the thermal conductivity of concrete; and increasing the content of polypropylene fiber significantly improves the mechanical properties of alkali-excited fly ash aerogel concrete. Ma R [20] used coal gangue and ground slag as raw materials and NaOH as an alkali activator to prepare a new type of cementing filler material. The results show that under the ratio of coal gangue 82.58%, alkali content 2.93% and slag content 30%, the main reaction products of backfill are C-S-H gel and C-A-S-H gel, and the performance of filling materials is the best. Lv X [21] found that industrial waste slag could be effectively used to prepare sand-alkali slag cementing material, and the results showed that steel fiber could effectively improve the mechanical properties of alkali slag cementing material. When the temperature is lower than $600 \text{ }^\circ\text{C}$, the steel fiber effectively improves the compressive and bending strength of the alkali slag cementing material. The main component of straw ash is SiO_2 , which can reach about 60%, and also contains Al_2O_3 , which has certain pozzolanic activity [22]. Raheem, AA [23] found that adding a proper amount of straw ash could reduce the thermal conductivity of cement. Nagrockiene D [24] found that replacing 10% cement with natural zeolite can increase the closed porosity, improve the compressive strength of concrete, and improve the freeze-thaw resistance of concrete. Tseng Y S [25] found that the incorporation of natural zeolite within 15% into cement-based materials could improve the early compressive strength.

In this paper, the problems of high heat loss and low heat recovery efficiency of shallow geothermal cementing cement during heat exchange in geothermal wells are studied. By adding thermal insulation materials, such as straw ash and natural zeolite, to replace a certain proportion of cement, and adding alkali activators, such as water glass, to stimulate the activity of cement-based materials, the thermal conductivity of cement is reduced and the mechanical properties of cement are guaranteed. The effects of alkali excitation materials on the macroscopic properties (compressive strength, thermal

conductivity, fluidity, thickening time) and microstructure (porosity and microstructure) of cement were studied.

The experiment employed a novel approach to modify the solid waste insulation material and conducted an orthogonal test, demonstrating higher efficiency, compared to the traditional method of incorporating a single insulation material. This study offers valuable guidance and recommendations for simultaneously enhancing the mechanical properties and insulation capabilities of geothermal well cement, while also introducing innovative ideas and methodologies for future research in this field.

2. Materials and Methods

2.1. Experimental Materials

The straw ash (manufactured by the Mengcheng Power Plant, located in Bozhou, China), is the combustion waste after combustion in the power plant, and the particle size is 200 mesh. The main component of natural zeolite (manufactured by the Yanxie Flagship Store, located in Henan, China) is SiO_2 , and the particle size is less than 200 mesh. The chemical composition of straw ash and natural zeolite is shown in Table 1. Grade G oil well cement is provided by Ningxia Qingtongxia Cement Co., LTD. (located in Qingtongxia, China). The physical properties are shown in Table 2.

Table 1. Chemical composition of thermal insulation materials.

| Thermal Insulation Materials | SiO_2 | Al_2O_3 | CaO | K_2O | Fe_2O_3 | NaO |
|------------------------------|----------------|-------------------------|------|----------------------|-------------------------|------|
| Straw ash | 52.42 | 7.05 | 5.97 | 12.55 | 4.62 | 1.45 |
| Natural zeolite | 74.44 | 14.96 | 1.35 | 5.14 | 1.10 | 1.83 |

Table 2. Physical performance of cement.

| Density (g/cm^3) | Specific Surface Area (m^2/kg) | Water: Cement Ratio | 35.6 MPa 52 °C | | 8 h Compressive Strength (MPa) | |
|------------------------------------|--|---------------------|------------------------------------|-----------------------|--------------------------------|-------|
| | | | 15–30 min Maximum Consistency (BC) | Thickening Time (min) | 38 °C | 60 °C |
| 3.18 | 349 | 0.44 | 18.9 | 108 | 5.9 | 16.2 |

The alkali activator used is industrial water glass (manufactured by Xi'an Huachang Water Glass Co., Ltd., located in Xi'an, China), and the water glass parameters are: Na_2O is 8.48%, SiO_2 is 27.13%, and the modulus is 3.2. The NaOH (manufactured by Tianjin Damao Chemical Reagent Factory, located in Tianjin, China) is white translucent flake/granular crystal. The content of NaOH is not less than 96.0%, and the carbonate (Na_2CO_3) is less than 1.5%. The water glass parameters are adjusted by calculating the amount of water glass and NaOH. Water reducer: polycarboxylic acid water reducer (manufactured by the Shanghai Chenqi Chemical Technology Co., Ltd., located in Shanghai, China), retarding agent: sodium gluconate (manufactured by the Shandong Yousuo Chemical Technology Co., Ltd., located in Linyi, China).

2.2. Orthogonal Design of Experiment

In this experiment, water glass with alkali equivalent of 8% and modulus of 1.8 was used for an orthogonal test. However, because the alkali equivalent and modulus of water glass were too large, the viscosity of cement slurry was too large, and the mixing water and materials were in a dry state and could not be stirred into slurry. Therefore, the alkali equivalent of water glass was 5%, 6% and 7%, and the modulus was 1.2, 1.4 and 1.6.

Straw ash (5%, 10%, and 15%), natural zeolite (5%, 10%, and 15%), water glass modulus (1.2, 1.4, and 1.6), and water glass alkali equivalent (5%, 6%, and 7%) were used to design orthogonal tests with four factors and three levels, as shown in Table 3.

Table 3. The proportion of orthogonal experimental.

| No. | A% Straw Ash | B% Natural Zeolite | C Water Glass Modulus | D% Water Glass Alkali Equivalent | Cement/g | Water Reducer/g | Water/g |
|-----|-----------------|--------------------------|-----------------------------|--|----------|--------------------|---------|
| C0 | 0 | 0 | 0 | 0 | 792.00 | 0 | 349.00 |
| Z1 | 15 | 10 | 1.2 | 7 | 594.00 | 2.376 | 349.00 |
| Z2 | 15 | 15 | 1.4 | 5 | 554.40 | 2.376 | 349.00 |
| Z3 | 10 | 5 | 1.4 | 7 | 673.20 | 2.376 | 349.00 |
| Z4 | 10 | 15 | 1.2 | 6 | 594.00 | 2.376 | 349.00 |
| Z5 | 10 | 10 | 1.6 | 5 | 633.60 | 2.376 | 349.00 |
| Z6 | 5 | 15 | 1.6 | 7 | 633.60 | 2.376 | 349.00 |
| Z7 | 5 | 5 | 1.2 | 5 | 712.80 | 2.376 | 349.00 |
| Z8 | 15 | 5 | 1.6 | 6 | 633.60 | 2.376 | 349.00 |
| Z9 | 5 | 10 | 1.4 | 6 | 673.20 | 2.376 | 349.00 |

2.3. Experimental Method

2.3.1. Preparation of Cement Paste

Referring to the “Oil Well Cement” GB/T 10238-2015 [26], prepare the thermal insulation cement, and cure the cement paste at 38 °C and 60 °C under atmospheric pressure. Pour the measured 349.00 g mixing water into the mixer cup and stir at a low speed at 4000 ± 200 r/min. Pour the fully mixed admixture and cement (792.00 g in total) into the mixing cup within 15 s and cover the lid. Then continue mixing at a high speed of 12,000 ± 500 r/min for 35 s, turn off the mixer instrument, open the lid, check if the cement slurry is fully stirred and the cement slurry system is completed, and use a glass rod to stir the cement slurry to prevent the cement slurry from thickening.

Preparation of compressive strength test block: Set the curing box temperature in advance and heat up to 38 °C and 60 °C, pour the prepared cement slurry into the copper mold (50 mm × 50 mm × 4 mm) within 5 min, pour the cement slurry to half of the mold first, use the glass vibrator to vibrate 17 times, and then fill the mold with the remaining cement slurry until it overflows. Use the glass vibrator to vibrate the cement paste 17 times again, use a scraper to scrape off the excess paste, cover the dry and clean cover plate, and tighten the screws. The cement paste is cured in water bath at 38 °C and 60 °C for 8 h and 28 d, respectively.

Thermal conductivity test block preparation: the prepared slurry is injected into the copper test mold within 2 min. First, it was cured at room temperature for 24 h, and then it was demolded into a standard curing box (temperature 20 °C, humidity 95%) for 28 d. After curing, the surface of the thermal conductivity test block was polished and smooth with 80 mesh sandpaper and 400 mesh sandpaper respectively, and then the thermal conductivity was determined to reduce the adverse impact on the thermal conductivity test.

2.3.2. Performance Tests of Cement Paste

Compressive strength. YAW-300 (manufactured by the Shaoxing Kent Machinery & Electronics Co., Ltd., located in Shaoxing, China) was used to determine the compressive strength of the insulation cement samples. The test parameters were as follows: the compression rate was 1.2 kN/s, and each group of cement samples was not less than 4 samples.

Thermal conductivity test. TC 3100 (manufactured by the Xi’an Xiaxi Electronic Technology Co., Ltd., located in Xi’an, China) was used to test the thermal conductivity of cement samples, and the error of heat balance detection was less than 0.1. The test

temperature of the thermal conductivity test block was 30 °C, 60 °C and 90 °C respectively, and the test times of each group of samples were not less than 4 times.

Flow: Put the flow test mold of cement paste on a dry and clean glass plate, quickly pour the prepared paste into the test mold, scrape the excess paste on the surface of the test mold with a scraper, and then quickly pick up the test mold vertically. After the cement paste no longer spreads outward, the diameter of the paste is measured vertically twice with a vernier caliper and the data is recorded.

Thickening time. According to the testing standards and requirements of GB/T 10238-2015 “Oil Well cement”, the prepared cement slurry is poured into the slurry cup of the pressurized thickener within 20 s to seal quickly, and then put into the pressurized thickener. After the sample was prepared, the pressurization thickener was set on the equipment. The circulating temperature was 52 °C, the circulating pressure was 35.6 MPa, and the heating and pressure boosting time was 28 min.

Porosity: The Micromeritics Auto Pore IV 9500 (manufactured by the American Mike Instrument Company, located in Atlanta, GA, USA) mercury intrusion meters from the United States. The testing aperture range is 0.005–800 µm.

SEM: Thin slices of about 1 cm × 1 cm in size and flat on both sides were selected before the sample fragments were pulverized for SEM scanning electron microscope testing. The German ZEISS Sigma300 (manufactured by the Karl Zeiss AG, Germany, located in Jena, Germany) scanning electron microscope. Magnification range: 25~200,000 times, Resolution: 1.2 nm, tested on thin sheet cement samples at 20 °C, magnification: 5 KX.

3. Results

3.1. Compressive Strength Analysis of Cement Pastet Based on Orthogonal Test

The compressive strength of the orthogonal test is shown in Table 4, and the compressive strength range analysis is shown in Table 5. It can be seen from Table 5 that under the conditions of curing at 38 °C and 60 °C for 8 h and 28 d, respectively, the range of water glass alkali equivalent is the largest, indicating that water glass alkali equivalent has the most significant influence on compressive strength.

Table 4. Table of compressive strength of orthogonal test.

| No. | 8 h Compressive Strength/MPa | | 28 d Compressive Strength/MPa | |
|-----|------------------------------|-------|-------------------------------|-------|
| | 38 °C | 60 °C | 38 °C | 60 °C |
| C0 | 7.64 | 18.50 | 54.11 | 66.23 |
| Z1 | 6.76 | 16.18 | 54.83 | 61.16 |
| Z2 | 4.50 | 13.88 | 48.94 | 57.38 |
| Z3 | 9.80 | 19.56 | 58.78 | 71.96 |
| Z4 | 5.38 | 14.86 | 54.71 | 64.64 |
| Z5 | 4.44 | 12.58 | 49.32 | 56.02 |
| Z6 | 9.26 | 24.46 | 57.39 | 70.46 |
| Z7 | 2.78 | 12.72 | 46.26 | 59.48 |
| Z8 | 5.26 | 15.68 | 52.84 | 60.36 |
| Z9 | 4.94 | 15.4 | 54.88 | 66.82 |

According to the range analysis table of orthogonal test for compressive strength in Table 5, under the conditions of curing at 38 °C for 8 h and 28 d, the influencing factors on the compressive strength of cement samples are ranked as follows: D (alkali equivalent) > C (water glass modulus) > A (straw ash) > B (natural zeolite). Under the conditions of curing at 6 °C for 8 h, the influencing factors on the compressive strength of cement samples are ranked as follows: D > C > B > A. Under the conditions of curing at 60 °C for 28 d the influencing factors on the compressive strength of cement samples are ranked as follows: D > A > C > B. When cured at both 38 °C for 8 hand 60 °C for 28 d, it is observed that sodium silicate base equivalent has a significantly larger range value, compared to sodium

silicate modulus, straw ash, and natural zeolite. This indicates that sodium silicate base equivalent is considered to the most significant factor among these four influencing factors in terms of compressive strength, and plays a crucial role.

Table 5. Compressive strength range analysis by orthogonal test.

| Index | | Factor | | | |
|--|-----------------|--------|-------|-------|-------|
| | | A | B | C | D |
| 38 °C 8 h compressive strength/MPa | K1 ¹ | 5.66 | 5.95 | 4.92 | 3.89 |
| | K2 ² | 6.54 | 5.38 | 6.41 | 5.19 |
| | K3 ³ | 5.50 | 6.38 | 6.32 | 8.61 |
| | R ⁴ | 1.04 | 1.00 | 1.40 | 4.72 |
| 60 °C 8 h compressive strength/MPa | K1 | 17.53 | 15.99 | 14.59 | 13.06 |
| | K2 | 15.67 | 14.72 | 16.28 | 15.31 |
| | K3 | 15.48 | 17.73 | 17.57 | 20.07 |
| | R | 2.05 | 3.01 | 3.02 | 7.01 |
| 38 °C 28 d compressive strength/MPa | K1 | 52.84 | 52.63 | 51.93 | 48.17 |
| | K2 | 54.27 | 53.01 | 54.2 | 54.14 |
| | K3 | 52.20 | 53.68 | 53.18 | 57 |
| | R | 2.07 | 1.05 | 2.27 | 8.83 |
| 60 °C 28 d compressive strength/MPa | K1 | 65.59 | 63.93 | 61.76 | 57.63 |
| | K2 | 64.21 | 61.33 | 65.39 | 63.94 |
| | K3 | 59.63 | 64.16 | 62.28 | 67.86 |
| | R | 5.96 | 2.83 | 3.63 | 10.23 |

¹ K1: The average value of a factor at level 1. ² K2: The average value of a factor at level 2. ³ K3: The average value of a factor at level 3. ⁴ R: The range of the average value of a factor at three levels.

As can be seen from Figures 1–4, under the condition of curing at 60 °C for 8 h, the compressive strength of cement paste increases with the increase of water glass modulus. Under the conditions of curing at 38 °C for 8 h, and at 38 °C and 60 °C for 28 d, the compressive strength of the cement paste first increased and then decreased with the increase of water glass modulus. When the water glass modulus is 1.2, the $[\text{SiO}_4]^{4-}$ in the solution is less, and the C-S-H gel generated by the reaction with Ca^{2+} is reduced, so the compressive strength of the cement paste is reduced. When the water glass modulus is 1.4, the $[\text{SiO}_4]^{4-}$ in the solution is moderate, the hydration reaction of the cement paste can proceed normally, the amount of C-S-H gel generated increases, and the compressive strength increases. When the water glass modulus is 1.6, it is too high, and the modulus will increase the consistency of the cement paste, and the mixing water and cement cannot be fully mixed. As a result, the hydration of the cement paste cannot be completely carried out, fewer products will be produced, and the compressive strength of cement will be reduced.

Under the condition of curing at 38 °C and 60 °C for 8 h, and at 60 °C for 28 d, the compressive strength of the cement paste first increased and then decreased with the increase of natural zeolite content. Under these four curing conditions, the compressive strength of cement paste also showed a trend of first increasing and then decreasing with the increase of straw ash content. This is because straw ash and natural zeolite are a kind of porous material, which can fill the pores of cement paste and increase the compressive strength of cement. When the content is large, the filling effect of straw ash and natural zeolite on cement paste is insufficient to make up for the compressive strength generated by cement hydration.

The compressive strength of cement paste increases with the increase of water glass equivalent concentration. With the increase of water glass equivalent, the hydration reaction rate is accelerated, and the C-S-H gel produced can promote the development of compressive strength. When the alkali equivalent is higher, OH^- enhances the dissoci-

ation and hydration activity of natural zeolite and straw ash, which is conducive to the development of compressive strength of cement paste.

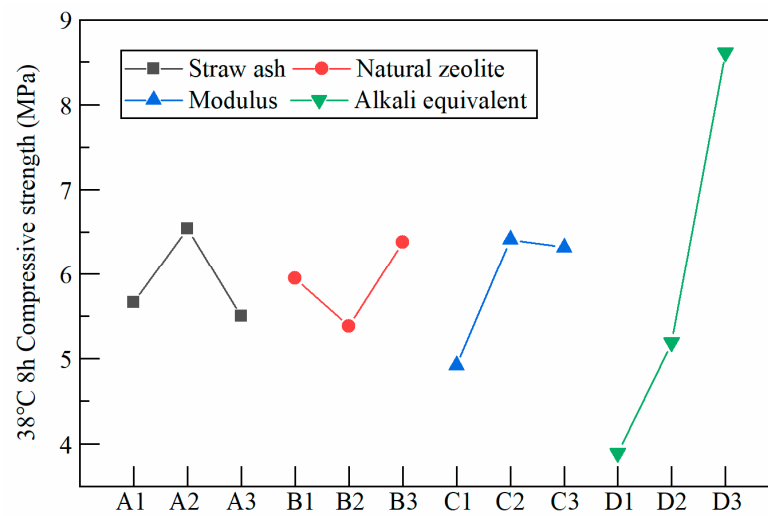


Figure 1. Trend diagram of influence of each factor level on compressive strength of cement paste cured at 38 °C for 8 h.

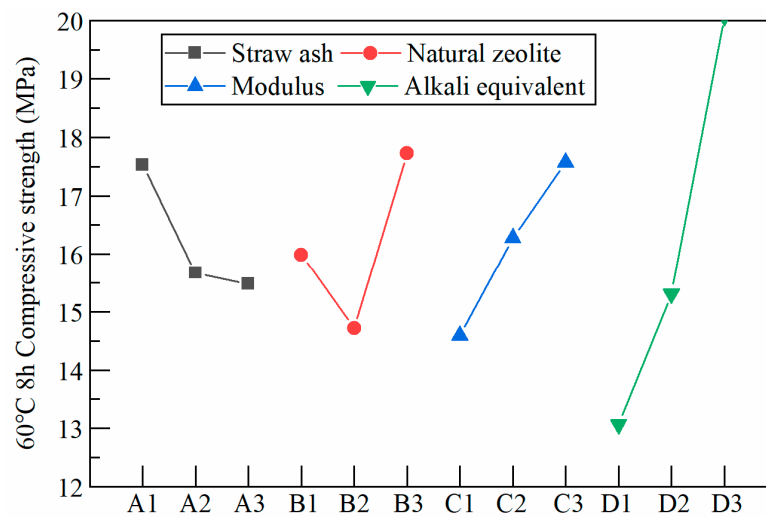


Figure 2. Trend diagram of influence of each factor level on compressive strength of cement paste cured at 60 °C for 8 h.

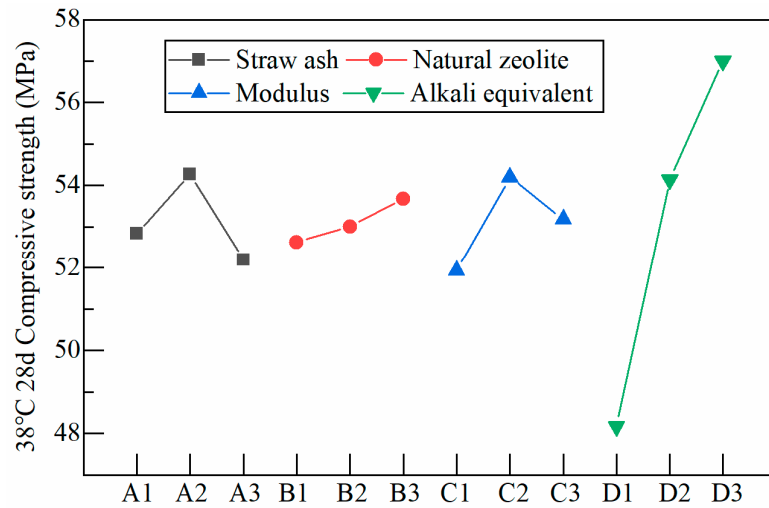


Figure 3. Trend diagram of influence of each factor level on compressive strength of cement paste cured at 38 °C for 28 d.

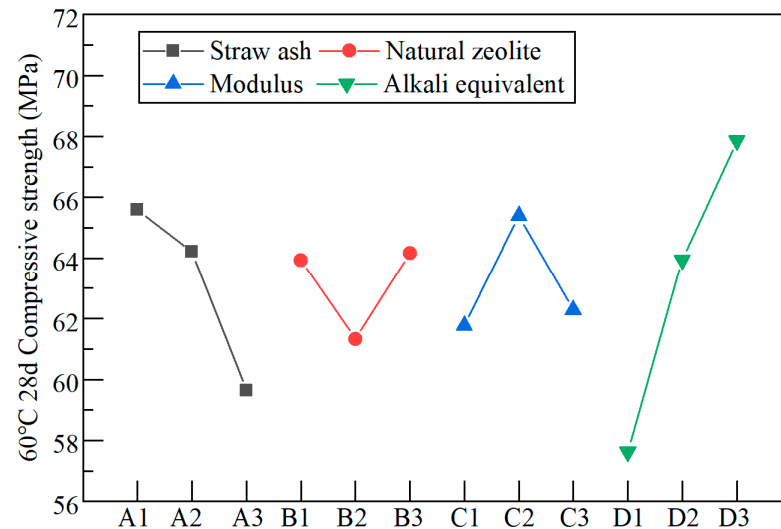


Figure 4. Trend diagram of influence of each factor level on compressive strength of cement paste cured at 60 °C for 28 d.

3.2. Thermal Conductivity Analysis of Cement Paste Based on Orthogonal Test

The thermal conductivity of the orthogonal test is shown in Table 6, and the thermal conductivity range analysis is shown in Table 7. As can be seen from Table 7, when the test temperature is 30 °C, the influencing factors on the thermal conductivity of cement paste are as follows: B > D > A > C; When the temperature is 60 °C, the influencing factors on the thermal conductivity of cement paste are as follows: B > C > D > A; When the temperature is 90 °C, the influencing factors on the thermal conductivity of cement paste are as follows: C > B > D > A.

Table 6. Table of thermal conductivity of orthogonal test.

| No. | Thermal Conductivity W/(m·K) | | |
|-----|------------------------------|--------|--------|
| | 30 °C | 60 °C | 90 °C |
| C0 | 0.8218 | 0.7718 | 0.7279 |
| Z1 | 0.5399 | 0.5134 | 0.4712 |
| Z2 | 0.4868 | 0.4341 | 0.3459 |
| Z3 | 0.7649 | 0.5057 | 0.4651 |
| Z4 | 0.6957 | 0.4896 | 0.473 |
| Z5 | 0.5468 | 0.5094 | 0.3798 |
| Z6 | 0.4733 | 0.3837 | 0.3346 |
| Z7 | 0.8351 | 0.5499 | 0.5367 |
| Z8 | 0.7156 | 0.5035 | 0.4354 |
| Z9 | 0.7831 | 0.5292 | 0.5227 |

At 30 °C and 60 °C, natural zeolite has the greatest influence on the thermal conductivity of cement paste and, with the increase of natural zeolite content, the thermal conductivity of cement decreases—because natural zeolite is a porous structural material, filling in cement paste can increase the heat transfer resistance of cement, and effectively reduce the thermal conductivity of cement paste.

At 90 °C, the biggest influence on the thermal conductivity of cement paste is the water glass modulus. With the increase of the water glass modulus, the thermal conductivity of cement decreases, the water glass modulus increases, and the content of $[\text{SiO}_4]^{4-}$ in the solution increases, which promotes the hydration reaction of cement and generates more C-S-H gel. C-S-H is a disordered and complex structure. It can form high thermal resistance structures of different sizes with natural zeolite and straw ash particles, improve the thermal resistance of cement and reduce the thermal conductivity. In addition, water glass is a gel substance, which has a low thermal conductivity, so the thermal conductivity of the cement paste is reduced.

Table 7. Thermal conductivity range analysis by orthogonal test.

| Index | | Factor | | | |
|---------------------------------------|----|--------|--------|--------|--------|
| | | A | B | C | D |
| 30 °C Thermal conductivity W/(m·K) | K1 | 0.6972 | 0.7719 | 0.6902 | 0.6229 |
| | K2 | 0.6691 | 0.6233 | 0.6783 | 0.7315 |
| | K3 | 0.5808 | 0.5519 | 0.5786 | 0.5927 |
| | R | 0.1164 | 0.2200 | 0.1116 | 0.1388 |
| 60 °C Thermal conductivity W/(m·K) | K1 | 0.4879 | 0.519 | 0.5186 | 0.4983 |
| | K2 | 0.502 | 0.5173 | 0.4883 | 0.5067 |
| | K3 | 0.4823 | 0.4359 | 0.4656 | 0.4672 |
| | R | 0.0197 | 0.0831 | 0.0530 | 0.0511 |
| 90 °C Thermal conductivity W/(m·K) | K1 | 0.4647 | 0.4791 | 0.4936 | 0.4208 |
| | K2 | 0.4393 | 0.4579 | 0.4446 | 0.477 |
| | K3 | 0.4175 | 0.3845 | 0.3832 | 0.4236 |
| | R | 0.0472 | 0.0946 | 0.1104 | 0.0562 |

It can be seen from Figures 5–7 that at the test temperatures of 30 °C, 60 °C and 90 °C, the thermal conductivity of the cement paste decreases with the increase of the content of straw ash and natural zeolite. Because both straw ash and natural zeolite are porous materials, adding straw ash and natural zeolite to cement can increase the porosity of cement paste, increase the thermal resistance of cement heat transfer, and reduce the thermal conductivity. With the increase of water glass modulus, the thermal conductivity of cement samples decreases, which is due to the increase of water glass modulus and the increase of $[\text{SiO}_4]^{4-}$ content in the solution, which promotes the hydration of cement and generates more C-S-H gel. The thermal conductivity of gel is lower than that of a solid, which can effectively reduce the thermal conductivity of cement. With the increase

of water glass alkali equivalent, the thermal conductivity of cement first increases and then decreases. When the alkali equivalent is too low, the alkali excitation effect of water glass on straw ash and natural zeolite is weak, and the cement hydration is not promoted. When the alkali equivalent is 6%, water glass contacts with straw ash and natural zeolite, and the OH⁻ ion in the solution starts to stimulate the vitreous structure in straw ash and natural zeolite. Due to the slow dissolution rate of ions at this time, the initially generated C-S-H may surround the straw ash and natural zeolite, hindering and slowing down the hydration rate and process of cement. When the alkali equivalent is 7%, the dissociation effect of OH⁻ in the solution on the straw ash and natural zeolite is enhanced, promoting the hydration of cement, and the generation of C-S-H is increased, which is beneficial to reducing the thermal conductivity of cement.

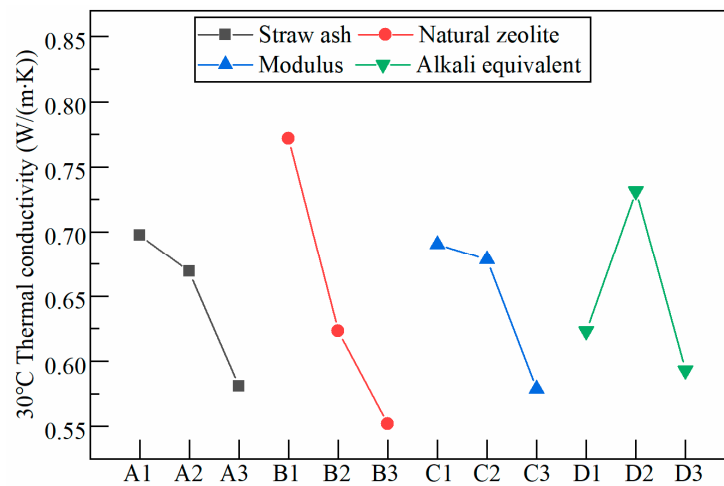


Figure 5. Trend diagram of influence of each factor level on thermal conductivity of cement paste tested at 30 °C.

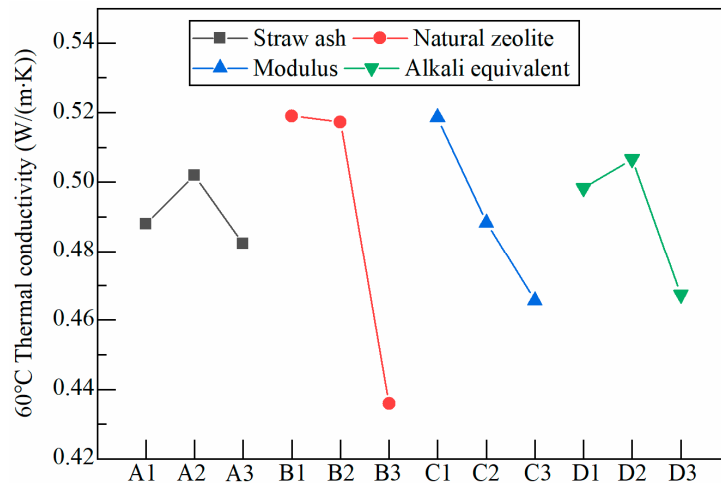


Figure 6. Trend diagram of influence of each factor level on thermal conductivity of cement paste tested at 60 °C.

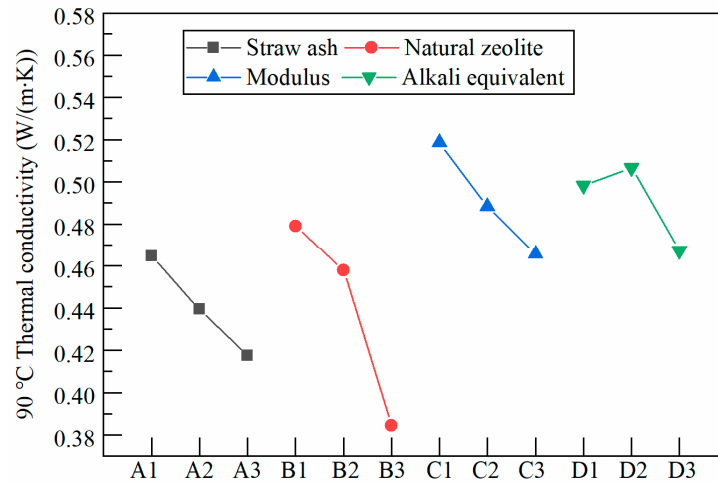


Figure 7. Trend diagram of influence of each factor level on thermal conductivity of cement paste tested at 90 °C.

3.3. Fluidity Analysis of Cement Paste Based on Orthogonal Test

The fluidity of the orthogonal test is shown in Table 8, and the range analysis of fluidity is shown in Table 9. As can be seen from Table 9, the influential factors of fluidity of cement paste are as follows: B > A > C > D, and natural zeolite has the greatest influence on fluidity of cement paste. It can be seen from Table 9 that the fluidity of cement samples in groups Z2 and Z5 is lower than 14 cm, which cannot meet the requirements of cementing construction. The common denominator of these two groups is that they contain 15% natural zeolite.

As can be seen from Figure 8, the fluidity of cement slurry decreases with the increase of natural zeolite content. Natural zeolite has a strong secretion, which will adsorb a lot of mixing water when mixed into cement, so that the free water used for cement mixing is reduced, so the fluidity of cement slurry is reduced. Straw ash also has certain water absorption due to its porous structure, and will also adsorb free water in the cement slurry, with the fluidity increasing first and then decreasing with the increase of straw ash content and water glass modulus. When the modulus of water glass is too large, the cement slurry becomes viscous and the fluidity decreases. Fluidity decreases first and then increases with the increase of water glass equivalent. The effect of water glass alkali equivalent on the flow of cement paste is small.

Table 8. Table of fluidity of orthogonal test.

| No. | Factor | | | | Fluidity/cm |
|-----|--------|-------|-----|-------|-------------|
| | A (%) | B (%) | C | D (%) | |
| C0 | 0 | 0 | 0 | 0 | 14.92 |
| Z1 | 15 | 10 | 1.2 | 7 | 15.97 |
| Z2 | 15 | 15 | 1.4 | 5 | 12.78 |
| Z3 | 10 | 5 | 1.4 | 7 | 21.06 |
| Z4 | 10 | 15 | 1.2 | 6 | 14.92 |
| Z5 | 10 | 10 | 1.6 | 5 | 15.17 |
| Z6 | 5 | 15 | 1.6 | 7 | 13.84 |
| Z7 | 5 | 5 | 1.2 | 5 | 19.06 |
| Z8 | 15 | 5 | 1.6 | 6 | 14.57 |
| Z9 | 5 | 10 | 1.4 | 6 | 16.85 |

Table 9. Fluidity range analysis by orthogonal test.

| Index | Factor | | | | |
|-------------|--------|-------|-------|-------|-------|
| | A | B | C | D | |
| Fluidity/cm | K1 | 16.58 | 18.23 | 16.65 | 15.67 |
| | K2 | 17.05 | 16.00 | 16.90 | 15.45 |
| | K3 | 14.44 | 13.85 | 14.53 | 16.96 |
| R | 2.61 | 4.38 | 2.37 | 1.51 | |

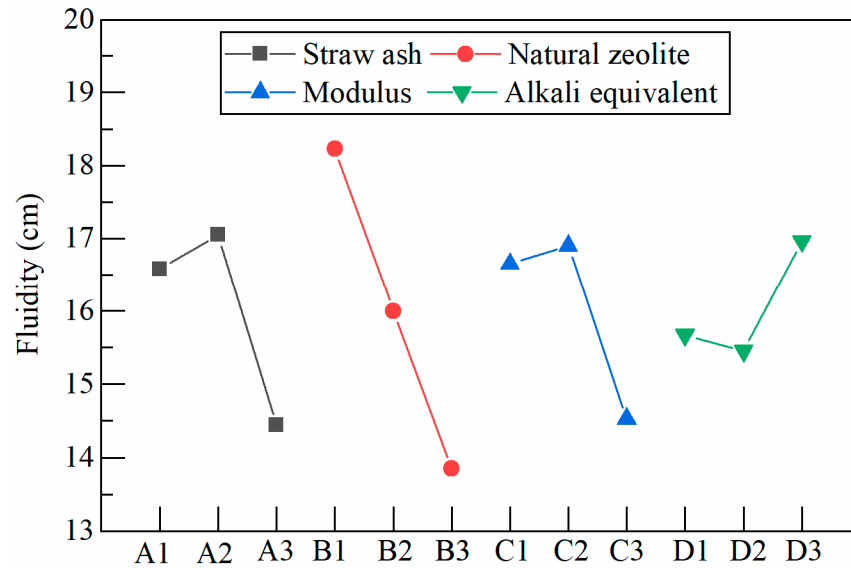


Figure 8. Trend diagram of influence of each factor level on fluidity of cement paste.

3.4. Comprehensive Evaluation

Analytic Hierarchy Process (AHP) is a hierarchical weight analysis method that combines qualitative and quantitative analysis. This method divides the problems to be analyzed into multiple indexes according to different hierarchical structures, and then assigns influence weight coefficient to each index by AHP analysis.

Compressive strength at 38 °C and 60 °C for 8 h, thermal conductivity tested at 30 °C and fluidity are used as reference indexes to evaluate the performance of cement. Since each indicator has a different unit dimension, it is impossible to directly evaluate each indicator. Therefore, in order to facilitate the evaluation of each indicator, it is necessary to eliminate the unit dimension and standardize the reference indicator (standard value = measured value/maximum value). In order to accurately evaluate the orthogonal test, the thermal conductivity of the cement paste is expressed by the thermal conductivity reduction rate (reduction rate = (maximum value – measured value)/maximum value), and then standardized.

According to the determination method of AHP index weight and the importance of the index, the four reference indexes are taken as four levels and the priority order is determined: thermal conductivity at 30 °C > compressive strength at 60 °C curing for 8 h > compressive strength at 38 °C curing for 8 h = fluidity. Yaahp12.2 software was used to calculate the comprehensive score of orthogonal tests: comprehensive evaluation = standard value of thermal conductivity at 30 °C × 0.7198 + compressive strength at 60 °C for 8 h × 0.1318 + compressive strength at 38 °C for 8 h × 0.0755 + fluidity × 0.0730.

The standard values and comprehensive scores of the orthogonal test are shown in Table 10, and the range analysis of comprehensive scores of the orthogonal test is shown in Table 11. According to Table 11, it can be seen that the sixth group of orthogonal test has the highest comprehensive score; that is, the best mix ratio of alkali-stimulated insulation

cement material is: Z6-A1B3C3D3; that is, when the content of cement is 80%, the content of straw ash is 5%, the content of natural zeolite is 15%, the use of parameters of water glass alkali equivalent is 7%, water glass modulus is 1.6 alkali activator, the comprehensive performance of cementing cement is the best.

Table 10. The standard value and comprehensive rating table of each index in the orthogonal test.

| No. | 38 °C 8 h Compressive Strength Standard Value | 60 °C 8 h Compressive Strength Standard Value | 30 °C Thermal Conductivity Reduction Rate % | 30 °C Thermal Conductivity Standard Value | Fluidity Standard Value | Comprehensive Score |
|-----|--|--|---|--|----------------------------|------------------------|
| Z1 | 68.98 | 66.15 | 29.97 | 81.60 | 75.83 | 78.20 |
| Z2 | 45.92 | 56.75 | 35.36 | 96.27 | 60.68 | 84.67 |
| Z3 | 100.00 | 79.97 | 7.13 | 19.41 | 100.00 | 39.36 |
| Z4 | 54.59 | 60.75 | 14.15 | 38.52 | 70.84 | 45.03 |
| Z5 | 45.31 | 51.43 | 29.27 | 79.69 | 72.03 | 72.82 |
| Z6 | 94.49 | 100.00 | 36.73 | 100.00 | 65.71 | 97.02 |
| Z7 | 28.37 | 52.00 | 0.00 | 0.00 | 90.50 | 15.60 |
| Z8 | 53.67 | 64.10 | 12.13 | 33.02 | 69.18 | 41.32 |
| Z9 | 50.41 | 62.96 | 5.28 | 14.38 | 80.01 | 28.30 |

Table 11. Comprehensive score range analysis table by orthogonal test.

| Index | Factor | | | | |
|----------------------|--------|-------|-------|-------|-------|
| | A | B | C | D | |
| Comprehensive rating | K1 | 46.97 | 32.09 | 46.28 | 57.70 |
| | K2 | 52.40 | 59.77 | 50.78 | 38.22 |
| | K3 | 68.06 | 75.57 | 70.39 | 71.53 |
| | R | 21.09 | 43.48 | 24.11 | 33.31 |

The compressive strength of Z6 cured at 38 °C and 60 °C for 8 h was 9.26 MPa and 24.46 MPa, respectively, which increased by 21.20% and 32.22%, compared with the pure cement. The compressive strength at 38 °C and 60 °C for 28 d was 57.39 MPa and 70.46 MPa, respectively, which increased by 6.51% and 6.39%, compared with the pure cement.

The thermal conductivity of Z6 measured at 30 °C, 60 °C and 90 °C is 0.4733 W/(m·K), 0.3837 W/(m·K), 0.3346 W/(m·K), and compared with the pure cement, the thermal conductivity reduction rates are 42.41%, 50.29% and 54.03%, respectively. According to some previous researches, the thermal conductivity of 20% expanded perlite and 20% hollow bleached beads thermal insulation cements were reduced by 19.0% and 13.4%, respectively [7]. The thermal conductivity of cement with 25% limestone was reduced by 36.26% [15]. The thermal conductivity of cement with 50% blast furnace slag was reduced by 35% [27].

According to the comprehensive score range analysis table, natural zeolite has the most significant influence on the comprehensive score of cement samples, followed by water glass alkali equivalent. Natural zeolite has complex pore structure and more pores, which can carry out ion adsorption on cement, improve cement bonding ability, increase thermal resistance in the process of electronic heat transfer and reduce heat loss in the insulation section of geothermal well.

3.5. Optimal Group Thickening Time

Test parameters of Group A: Z6 + 0.52% water reducer +0.8% retarder. The thickening time test of this ratio was carried out. Test conditions: The circulating temperature was 52 °C, the circulating pressure was 35.6 MPa, and the heating and pressure raising time was 28 min.

As shown in Figure 9, the initial temperature of the cement paste is 27.6 °C, the initial pressure is 5.3 MPa, the initial consistency is 22.2 BC, and the maximum consistency within 30 min is 22.2 BC less than 30 BC, which meets the requirements of the national standard, and the final thickening time is 93 min. With the increase of temperature and pressure, the cement consistency remained at about 22.2 BC within 60 min, and then rapidly increased to 100 BC within 33 min.

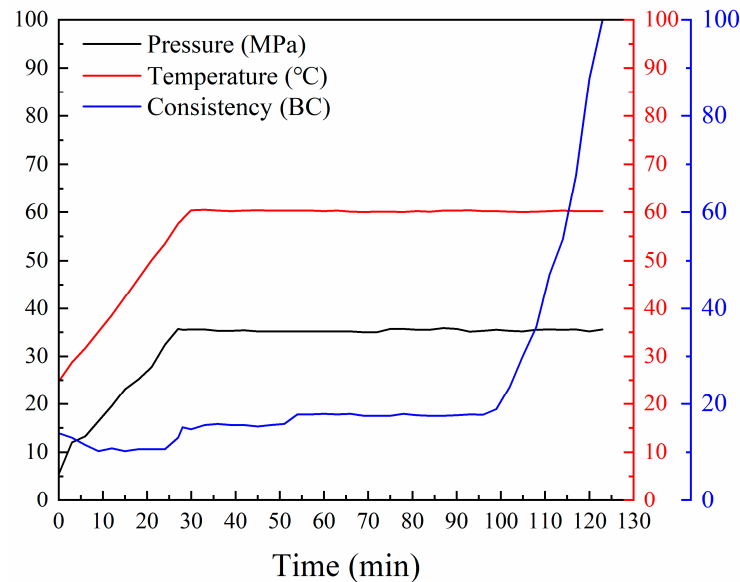


Figure 9. Curve of thickening time of A cement sample.

Test parameters of Group B: Z6 + 0.52% water-reducing agent +0.8% retarder. As shown in Figure 10, the initial temperature of the cement paste under this ratio is 24.8 °C, the initial pressure is 5.5 MPa, the initial consistency is 13.9 BC, the maximum consistency within 30 min is 15.1 BC less than 30 BC, meeting the requirements of the national standard, and the final thickening time is 123 min. The consistency of the cement paste remained within 18 BC before 96 min, after which the consistency increased rapidly and rose to 100 BC within 30 min.

Based on the thickening curves of the two groups of cement paste, it can be concluded that the thickening time of the initial consistency of alkali-fired cement can be adjusted by adjusting the content of water-reducing agent and retarder. Therefore, in the specific construction process, the content of water-reducing agent and retarder can be changed, according to the actual situation on site, to make the performance of cement paste meet the actual construction conditions.

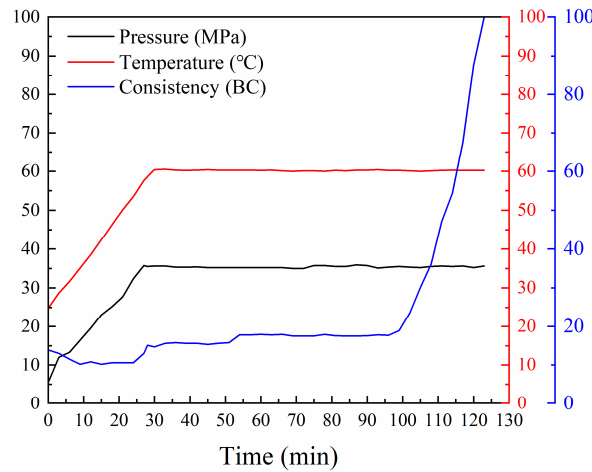


Figure 10. Curve of thickening time of B cement sample.

3.6. Optimal Group Porosity

Table 12 shows the distribution of porosity and pore class of THE Z6 sample with the optimal orthogonal ratio. It can be seen from the table that, compared with the pure cement, the porosity of Z6 decreased by 0.91%, the median pore size decreased by 69.84 nm, and the proportion of multi-damage pores was only 1.5% different from that of the pure cement—however, the low-damage pores were 34.77% lower than that of the pure cement, and the number of low-damage pores increased by 8.74%. The number of harmless holes increased by 26.53%. The multi-damage and harmful macropores are not favorable for the development of compressive strength of cement paste [28]. When these two kinds of pores are reduced, the density of cement paste is increased, and the compressive strength of cement samples is enhanced.

Table 12. Pore size distribution of Z6 cement sample.

| No. | Porosity/% | Median Aperture V/nm | Multi-Damage Pore/% | Harmful Pore/% | Less Damage Pore/% | Harmless Pore/% |
|-----|------------|----------------------|---------------------|----------------|--------------------|-----------------|
| C0 | 40.23 | 96.09 | 25.81 | 40.79 | 19.42 | 13.98 |
| Z6 | 39.12 | 26.25 | 24.31 | 6.02 | 28.16 | 41.51 |

It can be seen from the pore size distribution of Z6 cement sample and pure cement in Figure 11 that in the pore size < 50 nm, the distribution of Z6 is significantly more than that of pure cement, the porosity is reduced, and the harmless and less harmful pores are increased, indicating that alkali excitation of straw ash and natural zeolite can refine the pores and improve the compressive strength of cement paste.

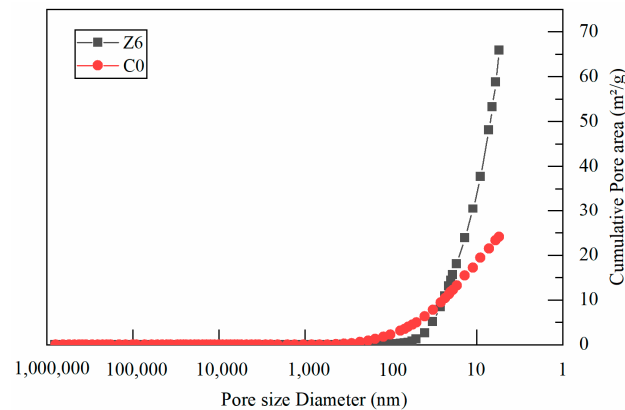


Figure 11. Pore size distribution of Z6 cement sample.

3.7. Microstructure of Optimal Group

Figure 12 shows the microstructure of cement paste after curing for 8 h and 28 d of Z6 in the optimal group of orthogonal.

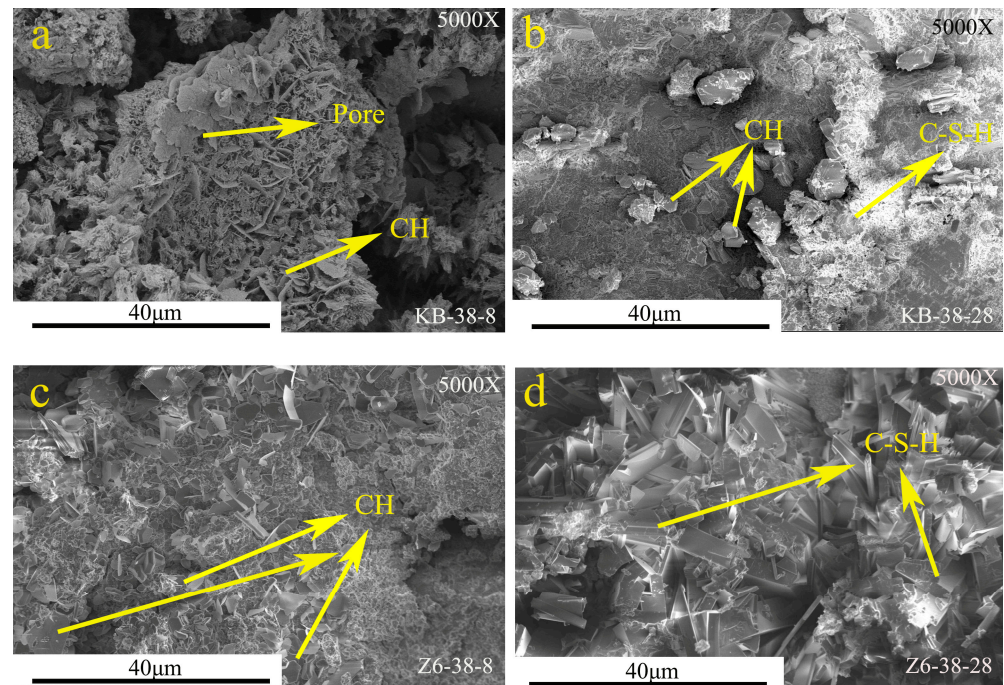


Figure 12. SEM images of the orthogonal optimal group cured at 38 °C for 8 h and 28 d: (a) C0—8 h; (b) C0—28 d; (c) Z6—8 h; (d) Z6—28 d.

Figure 12a shows the microstructure of pure cement sample after curing for 8 h at 38 °C; large cracks and many obvious pores can be seen in the figure, and the distribution of sheet $\text{Ca}(\text{OH})_2$, a primary hydration product of cement, in the cement paste can also be observed.

Figure 12b shows the microstructure of pure cement sample after curing for 28 d at 38 °C; it will be noted that there are almost no large holes in the cement paste, only a few small pores and micropores, the overall density of the cement paste is improved, and many hexagonal sheets of $\text{Ca}(\text{OH})_2$ and C-S-H are distributed in the cement paste, and stacked together to increase the density of cement.

Figure 12c shows the microscopic morphology of Z6 cement sample with optimal orthogonal mix ratio after curing at 38 °C for 8 h; Z6 generates more $\text{Ca}(\text{OH})_2$, indicating that the hydration reaction of cement paste can be promoted by using alkali activator, and a large amount of $\text{Ca}(\text{OH})_2$ is stacked together, reducing the porosity of cement paste. It makes the cement paste become denser and can improve the compressive strength of the cement paste.

Figure 12d shows the microscopic morphology of Z6 after curing at 38 °C for 28 d; it can be observed that C-S-H whiskers are covered with cement paste, and C-S-H whiskers pile up with each other to fill the pores of slurry cement, and the overall density of cement paste is good.

Compared with Figure 12b,d, it can be seen that Z6 cement samples cured for 28 d generated more calcium silicate whiskers than pure cement, which had higher mechanical properties and high temperature resistance—that is, good thermal insulation performance. Compared with Figure 12c, hydration products of cement paste cured for 28 d are almost all hydrated calcium silicate whisker without $\text{Ca}(\text{OH})_2$, while hydration products of cement paste cured for 8 h are $\text{Ca}(\text{OH})_2$, indicating that the alkali-induced reaction between straw ash and natural zeolite will be more obvious in the later stage of cement hydration.

Moreover, alkali excitation can promote the reaction of SiO_2 in natural zeolite and straw ash with Ca(OH)_2 , the primary hydration product of cement, to produce C-S-H whisker, which provides mechanical properties and thermal insulation properties for cement paste.

A large amount of C-S-H gel was generated by alkali-activated thermal insulation cement after curing for 28 d. The primary hydration product Ca(OH)_2 of cement and the active component $-\text{Al}_2\text{O}_3$ in straw ash and natural zeolite generated C-S-H gel through pozzolans effect, which were stacked together to effectively fill the pores of cement paste and increase the compactness. Fibrous C-S-H gel has good hardness itself, and filling in cement paste can effectively improve the compressive strength of cement. Due to its complex and disordered structure, C-S-H gel has a low thermal conductivity, and the thermal conductivity of Ca(OH)_2 is also low, but the thermal conductivity of C-S-H is lower than that of Ca(OH)_2 . A large number of fibrous C-S-H gels are interlaced to form many irregular and high thermal resistance structures with different sizes and heights, which enhance phonon scattering and effectively reduce the thermal conductivity of cement. This is consistent with the results of compressive strength and thermal conductivity of Z6 cement samples.

4. Discussion

According to the microscopic analysis, a large number of hexagonal Ca(OH)_2 was generated by alkali-activated insulation cement after curing for 8 h, which piled together and filled the pores of the cement paste. The porosity of the cement paste was reduced, and the number of large pores with more harmful and harmful was significantly reduced, being transformed into small and harmless pores and micropores. The porosity was reduced and the cement paste became denser. It can effectively improve the mechanical properties of cement compressive strength. The main hydration product of cement Ca(OH)_2 and the active component $-\text{Al}_2\text{O}_3$ in straw ash and natural zeolite produce C-S-H gel through the volcanic ash effect. Because of its complex and disordered structure, the thermal conductivity of C-S-H gel is low. The fibrous C-S-H gels are intertwined, forming many high thermal resistance structures with irregular size and height, enhancing phonon scattering and effectively reducing the thermal conductivity of cement. This is consistent with the results of compressive strength and thermal conductivity of Z6 cement sample.

Previously, numerous researchers have conducted studies on the incorporation of single-mix straw ash and single-mix natural zeolite as partial substitutes for cement. These studies have revealed that the addition of a small amount of straw ash can enhance the compressive strength of cement [29,30]. However, an increase in the quantity of straw ash leads to a decrease in compressive strength, which aligns with the findings of this experiment. Contrary to previous research, it was observed that incorporating natural zeolite results in a reduction in cement's compressive strength [31,32]. When used alone, natural zeolite primarily acts as a filler; however, due to its lightweight and porous nature, it fails to compensate for the strength provided by cement hydration. Consequently, this creates paste with reduced compressive strength. In this study, water glass is employed as an alkali activator to stimulate the reactivity of natural zeolite and promote cement hydration. This accelerates the rate at which cement hydrates while facilitating volcanic ash effects from Ca(OH)_2 and active component Al_2O_3 , to generate more C-S-H gel and provide additional strength for cement.

In recent years, there are more and more studies on the use of solid waste as a thermal insulation material to prepare geothermal cement. The thermal insulation performance of geothermal cement prepared by using solid waste as a thermal insulation material has been improved, but the mechanical properties will be reduced [14,15,33], which will affect the cementing quality of geothermal wells. Most of the studies on geothermal cement are on the short-term mechanical properties, and do not consider the changes and effects of long-term mechanical properties. In this experiment, the use of alkali-activated straw ash-natural zeolite as a thermal insulation material to prepare geothermal cement greatly improves the thermal insulation performance, and its short-term and long-term

mechanical properties are also significantly improved, which can ensure the cementing quality. The fluidity and thickening time of the alkali-activated straw ash-natural zeolite thermal insulation cement were examined in this study to meet engineering construction requirements. Thickening time is an important performance indicator of geothermal cementing construction. However, almost no previous studies on geothermal cement mentioned the performance of thickening time of cement [34–36]. During the thickening process, no false setting or flash setting phenomena occurred, effectively preventing adverse effects on geothermal well cementing and ensuring high-quality cementing.

The present research utilizes water glass-activated straw ash-natural zeolite composite material to develop a novel thermal insulation material suitable for geothermal well applications within oil well cements. This innovative approach addresses issues related to low-strength traditional thermal insulation materials while effectively impeding heat transfer and enhancing overall thermal insulation performance. The utilization of alkali-activated solid waste not only improves thermal insulation capabilities but also offers an alternative method for effective solid waste management by reducing accumulation and landfilling practices detrimental to environmental sustainability. The alkali-activated straw ash-natural zeolite thermal insulation cement exhibits a significantly low thermal conductivity. When utilized in geothermal wells, it not only effectively mitigates heat loss in the middle and upper sections of the wells, thereby enhancing geothermal energy extraction efficiency, but also enhances cementing quality and extends the operational lifespan of these wells.

5. Conclusions

(1) In the orthogonal test, the main factor affecting the compressive strength of cement is the alkali equivalent of water glass, the main factor affecting the thermal conductivity of cement is natural zeolite, and the main factor affecting the flow of cement is natural zeolite.

(2) Through an analytic hierarchy process, the optimal mix ratio of orthogonal test is obtained as follows: The compressive strength of 5% straw ash +15% natural zeolite +7% alkali equivalent and 1.6 modulus water glass is 9.26 MPa and 24.46 MPa, when cured at 38 °C and 60 °C for 8 h, and 57.39 MPa and 70.46 MPa, when cured at 38 °C and 60 °C for 28 d, respectively. The reduction rates of thermal conductivity at 30 °C, 60 °C and 90 °C are 42.41%, 50.29% and 54.03%, respectively.

(3) The use of water glass alkali to stimulate natural zeolite can promote the volcanic ash effect between OH⁻ and SiO₂ in natural zeolite, generating more C-S-H gel, which can improve the compressive strength of cement. C-S-H is a disordered and complex structure, which can improve the thermal resistance of cement and reduce the thermal conductivity of cement.

Author Contributions: Conceptualization, Y.J. and Q.S.; methodology, Q.S.; software, Q.S., Y.X. and T.Z.; validation, Y.J., Q.S. and G.Z.; formal analysis, Q.S.; investigation, Q.S.; resources, Q.S.; data curation, Q.S., Y.X. and T.Z.; writing—original draft preparation, Q.S.; writing—review and editing, Y.J. and Q.S.; visualization, Q.S.; supervision, Y.J.; project administration, Y.J.; funding acquisition, Y.X. and T.Z. All authors have read and agreed to the published version of the manuscript.

Funding: This research was funded by the Key Laboratory of Coal Resources Exploration and Comprehensive Utilization, Ministry of Natural Resources, (Grant number :ZD2018-3).

Institutional Review Board Statement: Not applicable.

Informed Consent Statement: Not applicable.

Data Availability Statement: Data are contained within the article.

Conflicts of Interest: Author Gang Zhu was employed by the company China Building Materials Industry Construction Xi'an Engineering Limited company. Authors Yuze Xue and Tinghui Zhang were employed by the company Shaanxi Coal Geology Group Co., Ltd. The remaining author declares that the research was conducted in the absence of any commercial or financial relationships that could be construed as a potential conflict of interest.

References

1. Phuoc, T.X.; Massoudi, M.; Wang, P.; Mckoy, M.L. Heat losses associated with the upward flow of air, water, CO₂ in geothermal production wells. *Int. J. Heat Mass Transf.* **2019**, *132*, 249–258. [\[CrossRef\]](#)
2. Song, X.Z.; Zheng, R.; Li, R.X.; Li, G.S.; Sun, B.J.; Shi, Y.; Wang, G.S.; Zhou, S.J. Study on thermal conductivity of cement with thermal conductive materials in geothermal well. *Geothermics* **2019**, *81*, 1–11. [\[CrossRef\]](#)
3. Ebrahimi, M.; Torshizi, S. Optimization of power generation from a set of low-temperature abandoned gas wells, using organic Rankine cycle. *J. Renew. Sustain. Energy* **2012**, *4*, 866–872. [\[CrossRef\]](#)
4. Wu, B.S.; Zhang, X.; Jeffrey, R.G. A model for downhole fluid and rock temperature prediction during circulation. *Geothermics* **2014**, *50*, 202–212. [\[CrossRef\]](#)
5. Song, X.Z.; Zheng, R.; Li, G.S.; Shi, Y.; Wang, G.S.; Li, J.C. Heat extraction performance of a downhole coaxial heat exchanger geothermal system by considering fluid flow in the reservoir. *Geothermics* **2018**, *76*, 190–200. [\[CrossRef\]](#)
6. Shi, Y.; Song, X.Z.; Li, G.S.; Yang, R.Y.; Shen, Z.H.; Liu, Z.H. Numerical investigation on the reservoir heat production capacity of a downhole heat exchanger geothermal system. *Geothermics* **2018**, *72*, 163–169. [\[CrossRef\]](#)
7. Zhang, F.Y.; Li, L.X. Study on thermal conductivity of thermal insulation cement in geothermal well. *Front. Earth Sci.* **2022**, *10*, 784245. [\[CrossRef\]](#)
8. Abid, K.; Srivastava, S.; Tellez, M.L.R.; Teodoriu, C.; Amani, M. Experimental and machine learning study of thermal conductivity of cement composites for geothermal wells. *Geothermics* **2023**, *110*, 102659. [\[CrossRef\]](#)
9. Ichim, A.; Teodoriu, C.; Falcone, G. Influence of cement thermal properties on wellbore heat exchange. In Proceedings of the 41st Annual Stanford Geothermal Workshop, Stanford, CA, USA, 22–24 February 2016.
10. Song, X.Z.; Wang, G.S.; Shi, Y.; Li, G.S.; Li, R.X.; Xu, Z.M.; Zheng, R.; Wang, Y. Numerical Analysis of Heat Extraction Performance of a Deep Coaxial Borehole Heat Exchanger Geothermal System. *Energy* **2018**, *164*, 1298–1310. [\[CrossRef\]](#)
11. Choktawekarn, P.; Saengsoy, W.; Tangtermsirikul, S. A model for predicting thermal conductivity of concrete. *Mag. Concr. Res.* **2009**, *61*, 271–280. [\[CrossRef\]](#)
12. Qiang, L.K.; Wei, C.X.; Yong, M.; Shu, G.X.; Jin, Y.Y.; Mei, Z.C.; Yang, G.X.; Jia, Z. Visualization and quantification of pore structure of oil-well cement slurry in liquid-solid transition stage using high-resolution computed tomography. *Cem. Concr. Compos.* **2020**, *111*, 103633. [\[CrossRef\]](#)
13. Bu, Y.H.; Du, J.P.; Guo, S.L.; Liu, H.J.; Huang, C.X. Properties of oil well cement with high dosage of metakaolin. *Constr. Build. Mater.* **2016**, *112*, 39–48. [\[CrossRef\]](#)
14. Zhou, W.; Wang, C.; Meng, R.; Chen, Z.; Lu, H.; Chi, J. Study on thermal insulation cement and its thermal insulation characteristics for geothermal wells. *Sci. Rep.* **2023**, *13*, 4157. [\[CrossRef\]](#)
15. Du, Y.; Yang, W.; Ge, Y.; Wang, S.; Liu, P. Thermal conductivity of cement paste containing waste glass powder, metakaolin and limestone filler as supplementary cementitious material. *J. Clean. Prod.* **2021**, *287*, 125018. [\[CrossRef\]](#)
16. Rashad, A.M.; Essa, G.M.F.; Morsi, W.M. Traditional Cementitious Materials for Thermal Insulation. *Arab. J. Sci. Eng.* **2022**, *47*, 12931–12943. [\[CrossRef\]](#)
17. Jadhav, P.S.; Sarkar, A.; Pasupathy, S.; Ren, S. Biogenic Straw Aerogel Thermal Insulation Materials. *Adv. Eng. Mater.* **2023**, *25*, 2300037. [\[CrossRef\]](#)
18. An, L.; Armstrong, J.N.; Hu, Y.; Huang, Y.; Li, Z.; Zhao, D.; Sokolow, J.; Guo, Z.; Zhou, C.; Ren, S. High temperature ceramic thermal insulation material. *Nano Res.* **2022**, *15*, 6662–6669. [\[CrossRef\]](#)
19. Rong, X.; Zhang, X.; Zhang, J.; Xu, W.; Zhang, Z. Study on mechanical and thermal properties of alkali-excited fly ash aerogel foam concrete. *Constr. Build. Mater.* **2023**, *408*, 133770. [\[CrossRef\]](#)
20. Ma, R.; Wang, G.; Sun, Q. Preparation and strength formation mechanism of alkali-stimulated spontaneous combustion gangue-granulated blast furnace slag backfill. *Environ. Sci. Pollut. Res.* **2024**, *31*, 723–739. [\[CrossRef\]](#)
21. Lv, X.; Cheng, H.; Chen, P.; Li, Y.; Wang, Z. Compression and bending of alkali-activated slag cementitious materials at high temperature. *Mag. Concr. Res.* **2024**, *76*, 37–54. [\[CrossRef\]](#)
22. Salvo, M.; Rizzo, S.; Caldirola, M.; Novajra, G.; Canonico, F.; Bianchi, M.; Ferraris, M. Biomass ash as supplementary cementitious material (SCM). *Adv. Appl. Ceram.* **2015**, *114*, 3–10. [\[CrossRef\]](#)
23. Raheem, A.A.; Akinteye, I.A.; Lasisi, S.A. A study of thermal conductivity of wood ash blended cement mortar. *Pac. J. Sci. Technol.* **2014**, *12*, 261–267. [\[CrossRef\]](#)
24. Nagrockiene, D.; Girskas, G. Research into the properties of concrete modified with natural zeolite addition. *Constr. Build. Mater.* **2016**, *113*, 964–969. [\[CrossRef\]](#)
25. Tseng, Y.S.; Huang, C.L.; Hsu, K.C. The pozzolanic activity of a calcined waste FCC catalyst and its effect on the compressive strength of cementitious materials. *Cem. Concr. Res.* **2005**, *35*, 782–787. [\[CrossRef\]](#)
26. GB/T 10238-2015; Oil Well Cement. Standards Press of China: Beijing, China, 2015.
27. Demirboga, R. Thermo-mechanical properties of sand and high volume mineral admixtures. *Energy Build.* **2003**, *35*, 435–439. [\[CrossRef\]](#)
28. Yang, Y.; Wang, K.; Zhang, H.; Xu, S.; Zhang, W.; Han, Y.; Li, Y. Investigation on the preparation, properties, and microstructure of high thermal conductive cementing material in 3500 m-deep geothermal well. *Geothermics* **2022**, *100*, 102322. [\[CrossRef\]](#)
29. Yunita, L.; Irmaya, A.I. Effectivity additives of baggase, ash straw, and sawdust wood albasia to compressive strength drilling cement. *IOP Conf. Ser. Earth Environ. Sci.* **2018**, *212*, 012079. [\[CrossRef\]](#)

30. Salem, S.; Hamdy, Y.; Abdelraouf, E.-S.; Shazly, M. Towards sustainable concrete: Cement replacement using Egyptian cornstalk ash. *Case Stud. Constr. Mater.* **2022**, *17*, e01193. [[CrossRef](#)]
31. Kocak, Y.; Tascı, E.; Kaya, U. The effect of using natural zeolite on the properties and hydration characteristics of blended cements. *Constr. Build. Mater.* **2013**, *47*, 720–727. [[CrossRef](#)]
32. Alena, S.á.; Matej, p.; Mária, K.; Marek, K. Long-Term Properties of Cement-Based Composites Incorporating Natural Zeolite as a Feature of Progressive Building Material. *Adv. Mater. Sci. Eng.* **2017**, *2017*, 7139481. [[CrossRef](#)]
33. Shen, L.; Tan, H.; Ye, Y.; He, W. Using Fumed Silica to Develop Thermal Insulation Cement for Medium–Low Temperature Geothermal Wells. *Materials* **2022**, *15*, 5087. [[CrossRef](#)] [[PubMed](#)]
34. Zhang, H.; Xu, S.; Yang, Y.; Han, Y.; Zhang, W.; Li, Y. Influencing factors of thermal conductivity of cementing materials for geothermal wells. *Coal Geol. Explor.* **2020**, *48*, 195–201. [[CrossRef](#)]
35. Yang, Y.; Li, B.; Che, L.; Li, T.; Li, M.; Liu, P.; Zeng, Y.; Long, J. Study on the performance and mechanism of high thermal conductivity and low-density cementing composite for deep geothermal wells. *Energy* **2023**, *285*, 129429. [[CrossRef](#)]
36. Li, Y.; Wang, S.; He, X.; Xiang, J. Investigation of consolidation/thermal insulation property and mechanism of casing cement in the heat-insulating section of geothermal production well. *Energy Sources Part A Recovery Util. Environ. Eff.* **2023**, *45*, 11566–11585. [[CrossRef](#)]

Disclaimer/Publisher’s Note: The statements, opinions and data contained in all publications are solely those of the individual author(s) and contributor(s) and not of MDPI and/or the editor(s). MDPI and/or the editor(s) disclaim responsibility for any injury to people or property resulting from any ideas, methods, instructions or products referred to in the content.